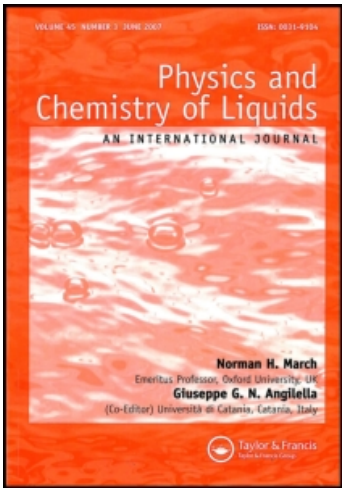

Physics and Chemistry of Liquids
Publication details, including instructions for authors and subscription information:
http://www.informaworld.com/smpp/title~content=t713646857

Structure of Dense Krypton Gas: Percus-Yevick and Monte Carlo Results

J. Ram[ab]; P. A. Egelstaff[a]
[a] Physics Department, University of Guelph, Guelph, Ontario, Canada [b] Department of Physics, Banaras Hindu University, Varanasi, India

To cite this Article Ram, J. and Egelstaff, P. A.(1984) 'Structure of Dense Krypton Gas: Percus-Yevick and Monte Carlo Results', Physics and Chemistry of Liquids, 14: 1, 29 — 45
To link to this Article: DOI: 10.1080/00319108408080793
URL: http://dx.doi.org/10.1080/00319108408080793

Phys. Chem. Liq., 1984, Vol. 14, pp. 29–46
0031-9104/84/1401–0029$18.50/0

Printed in the United Kingdom

Structure of Dense Krypton Gas: Percus-Yevick and Monte Carlo Results

J. RAM† and P. A. EGELSTAFF

Physics Department, University of Guelph, Guelph, Ontario, Canada N1G 2W1

(*Received November 30, 1983*)

Monte Carlo calculations of the pair correlation function $g(r)$ and numerical solutions of the Percus–Yevick equation are reported for a Lennard-Jones potential, the krypton potential of Barker *et al.* and a long range three-body (triple dipole and dipole-dipole-quadrupole) potential at 297 K and densities between 2 and 14 × 10^{27} atoms/m^3. We compare in real and Fourier space, and also calculate the pressure and compressibility. The latter two quantities are compared to experimental data on the 297 K isotherm, and while the PY results are in agreement the Barker *et al.* potential results are significantly different for $\rho > 3 \times 10^{27}$ atoms/m^3.

It is found that if the point where $u(r) = 0$ is chosen appropriately either Lennard-Jones or Barker *et al.* potential would yield a reasonable fit to the structure factor, $S(q)$, for $q > 2$ Å^{-1}. The shape of the attractive part of the potential influences $S(q)$ mainly for $q < 1$ Å^{-1}. Except at values of $q < 2$ Å^{-1} the effect of three-body forces on the structure factor is negligible at the state ($\rho = 14 \times 10^{27}$) studied here.

I INTRODUCTION

Recently Egelstaff and coworkers[1,8] have measured accurately the structure factor of gaseous krypton at various densities and compared it with Monte Carlo computations. They were able to extract some information about the range of many-body interactions and in a later paper[2] show that the contribution to $g(r)$ or $S(q)$ decreases with increasing density if a three-body potential having the Axilrod–Teller[4] form is used.

The computer simulation method has been used widely to study model fluids.[3] In this paper we report such calculations of the pair correlation

† On leave of absence from the Department of Physics, Banaras Hindu University, Varanasi-221005, India.

function $g(r)$ for dense krypton gas as a function of density along an isotherm. An attempt has been made to investigate the effect of a long-range three-body (triple dipole and dipole-dipole-quadrupole) potential on the short range part of $g(r)$. We shall present our results in Fourier space in order to suggest improvements to diffraction experiments and to interpret experimental data.[1,5]

The Lennard-Jones (12–6) (LJ) fluid has been widely studied by both theoretical and computer simulation methods.[6] Although the LJ model is known to be inaccurate as a representation of the intermolecular potential for inert gases,[6] it is sufficiently close to reality that the LJ fluid provides a convenient model for testing liquid theories and for investigating such phenomena as melting, the liquid-vapor interface, nucleation, etc. In this paper we compare LJ and Barker *et al.* fluids to find the relevant part of the two-body potential of interest in comparisons of absolute values with experiment. For the same reason in Section II we compare the LJ and krypton potential of Barker *et al.*[7] and their Percus–Yevick (PY) structure factors. For later comparison with experiment[1,8] we chose an isotherm at 297 K and densities between 2 and 14 $\times$ 10^{27} atoms/m^3.

Section III outlines our Monte Carlo calculations and its comparison with PY results for LJ and Barker *et al.* potentials. We present also calculations of the pressure and compressibility for these cases, and compare to real experimental results to show the effect on these properties of many body forces. In Section IV we have discussed the effect of three-body forces on the structure factor.

II PY STRUCTURE FACTORS FOR LJ AND BARKER *et al.* POTENTIALS

If the PY approximation

$$c(r) = g(r)[1 - \exp(\beta u(r))] \tag{1}$$

is combined with the Ornstein–Zernicke definition of the direct correlation function $c(r)$,

$$h(r) = c(r) + \rho \int c(r')h(|\mathbf{r} - \mathbf{r}'|)\, d\mathbf{r}', \tag{2}$$

where $\beta = 1/kT$, ρ is the number density, and $u(r)$ the intermolecular potential, then one obtains an integral equation for the radial distribution function $g(r)$. It is expedient to solve this equation by an iterative procedure. Convergence is enhanced by writing[9]

$$h_{\text{in}}^{(n+1)} = (1 - \alpha)h_{\text{out}}^{(n)} + \alpha h_{\text{out}}^{(n-1)} \tag{3}$$

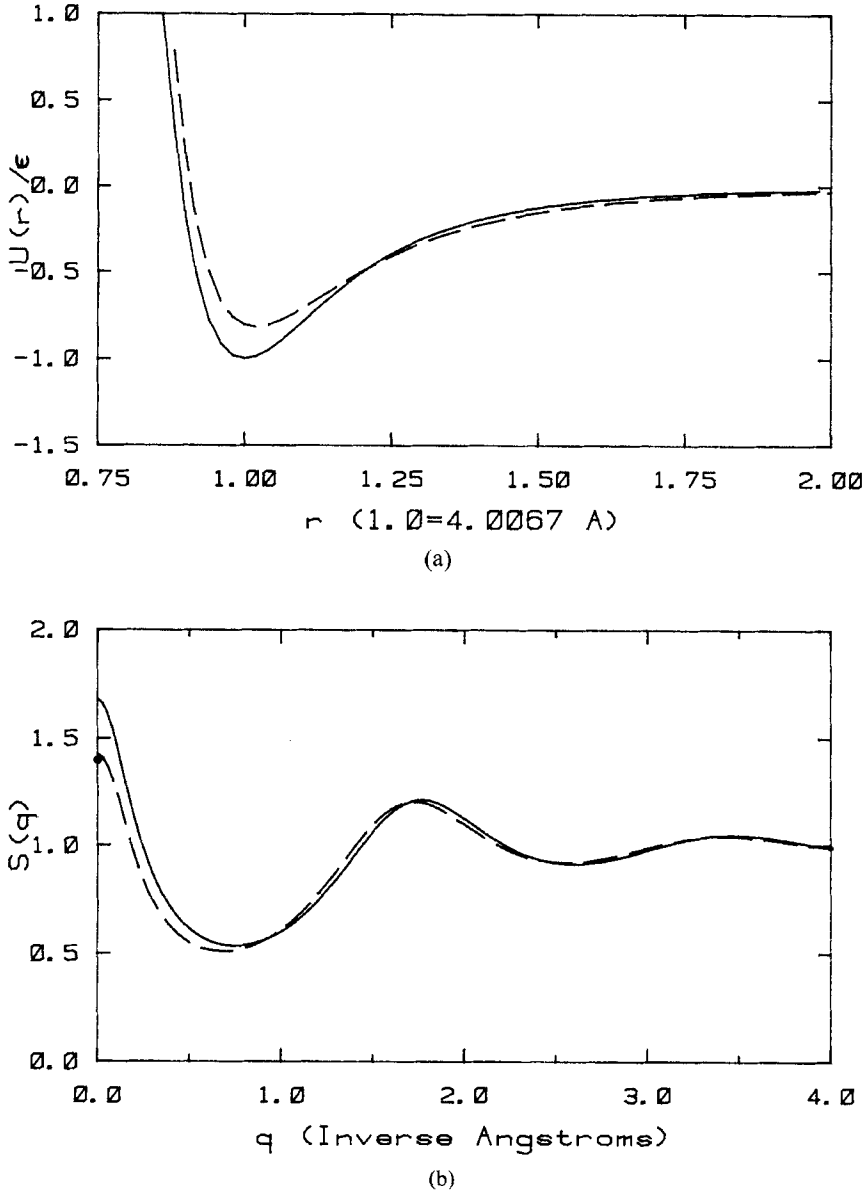

FIGURE 1 (a) The Barker *et al.*[7] potential for krypton as a full line and the Lennard-Jones potential deduced from the properties of the solid[10] as a dashed line. (b) The structure factors of krypton gas at 297 K and $\rho = 6 \times 10^{27}$ atoms/m^3 calculated from the Percus–Yevick equation using the two potentials shown in (a). The value of $S(o)$ calculated in Section IIIB is shown by the circle on the $S(q)$ axis.

where $h_{in}^{(n)}$ and $h_{out}^{(n)}$ are the nth input and output respectively and α is a mixing parameter. Starting with a trial h, we iterate until a self-consistent h is obtained. We used the following convergence criterion

$$|h^{(n+1)} - h^{(n)}| \leq 10^{-4} \tag{4}$$

The resulting numerical functions were Fourier transformed to find the structure factor $S(q)$, where

$$S(q) = 1 + \int \rho e^{i\mathbf{q}\cdot\mathbf{r}}[g(r) - 1]\, d\mathbf{r} \tag{5}$$

Figure 1 compares the LJ[10] and Barker *et al.*[7] krypton potentials and their PY structure factors at $T = 297$ K and $\rho = 6 \times 10^{27}$ atoms/m^3. The small shift between the two potentials at the position where $u(r) = 0$ (Figure 1a) causes the oscillations of $S(q)$ for $q > 1.5$ Å^{-1} to be slightly out-of-phase in Figure 1b. However the important differences occur for $q < 1.0$ Å^{-1} and are related to the differences of $u(r)$ in the range 4 Å $< r < 10$ Å. As this is the range over which both $u(r)$ and the three-body potential show important features, experimental measurements for $q < 1.0$ Å^{-1} need to be carried out carefully. In fact, if the point where $u(r) = 0$ is chosen appropriately, it appears from Figure 1 that the predictions of these two potentials would agree for $q > 1$ Å^{-1}. This conclusion is, of course, in accord with the results of perturbation theory. The differences at $q < 1$ Å^{-1} are made evident because the density is that of a gas. Because liquids are relatively incompressible for states near the triple point, their intensity for $q < 1$ Å^{-1} is low and the experimental data is so poor that this difference is not observed. Thus improved measurements on liquids for $q < 1$ Å^{-1} would be desirable to observe the difference between predictions based on different $u(r)$'s.

III MONTE CARLO STRUCTURE FACTORS COMPARED TO THE PERCUS–YEVICK APPROXIMATION

A Structure factors

The Monte Carlo calculations using the pair potential were carried out with a 500-particle system located in a cubical box. An NVT ensemble[7] and periodic boundary conditions were used. Fourteen states having densities between 2 and 14 $\times$ 10^{27} atoms/m^3 and a temperature of 297 K were simulated using the pair potential of Barker *et al.*[7] for krypton (K2) and runs of 300,000 configurations. Each simulation began with the particles being placed randomly with no overlap within the cubical box, and the first 25000 configurations were used to equilibrate the system. To monitor the calculation

for bottlenecks and an insufficient number of equilibrating configurations, the configurational energy and the mean squared displacement were examined every 5000 configurations. At the end, estimates of the average configuration energy and its uncertainty were obtained and compared with the energy obtained from the integral $\rho/2 \int g(r)u(r)\,dr$. The calculation was terminated when two methods gave agreement of (typically) less than 1 percent. Table I is a list of these $g(r)$ data.

In the Fourier transformation to find the structure factor from the Monte Carlo radial distribution function it is necessary to extrapolate the data to $R \to \infty$. For these cases the data were extrapolated beyond $R(= r/R_m) = 4.5$ up to $R = 8$ using the Percus–Yevick radial distribution function, and for $R > 8$ we set $g(r) = 1$. This introduces an error at low q in the Fourier space results, and therefore we shall not use these results for $q < 0.4$ Å^{-1}. We have also done similar Monte Carlo calculations for the LJ potential on three states (6, 11 and 14 $\times$ 10^{27} atoms/m^3).

Three examples of the resulting Monte Carlo and PY structure factors (at densities of 6, 11, and 14 $\times$ 10^{27} atoms/m^3) are shown in Figures 2, 3a,b and 4a,b. Figure 2 compares the Monte Carlo results corresponding to the

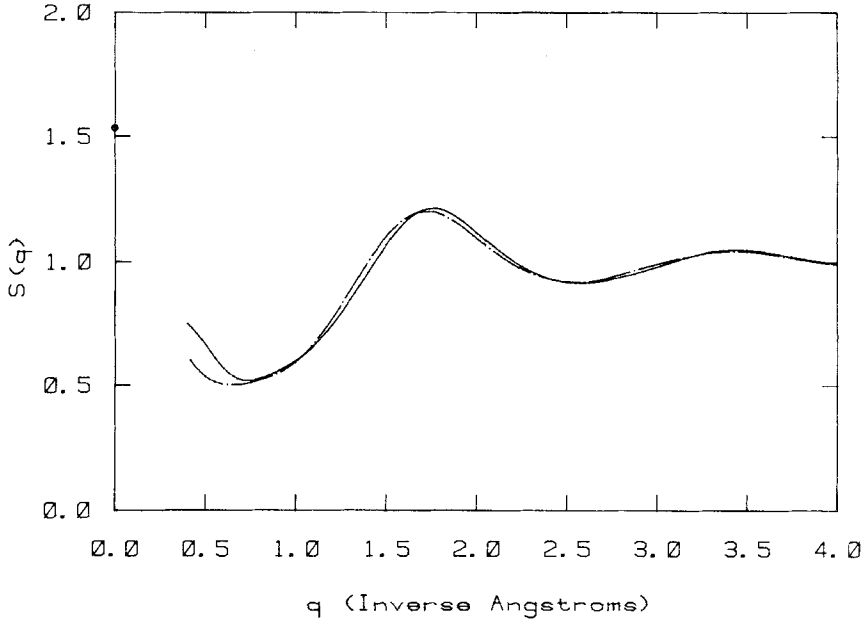

FIGURE 2 Monte Carlo structure factors for krypton at 297 K and $\rho = 6 \times 10^{27}$ atoms/m^3. The full line is simulated with Barker *et al.*[7] pair potential and long-dash-dot line is a simulation using Lennard-Jones potential. The value of $S(o)$ calculated in Section IIIB is shown by the circle on the $S(q)$ axis.

TABLE I

List of Monte Carlo $g(r)$'s for Barker *et al.*[7] (K2) potential at 297 K

	Density in units of 10^{27} atoms/m^3													
R/Rm	2.000	2.500	3.000	4.000	5.000	6.000	7.000	8.000	9.000	10.000	11.000	12.000	13.000	14.000
0.7502	0.0	0.0	0.0	0.0	0.0004	0.0	0.0000	0.0	0.0	0.0	0.0	0.0000	0.0002	0.0
0.7752	0.0010	0.0015	0.0007	0.0014	0.0023	0.0010	0.0007	0.0013	0.0007	0.0009	0.0016	0.0019	0.0026	0.0014
0.8002	0.0183	0.0219	0.0196	0.0202	0.0200	0.0198	0.0225	0.0204	0.0226	0.0224	0.0245	0.0239	0.0293	0.0310
0.8252	0.1045	0.1171	0.1063	0.1147	0.1056	0.1053	0.1142	0.1161	0.1112	0.1248	0.1293	0.1386	0.1537	0.1649
0.8502	0.3188	0.3186	0.3409	0.3249	0.3440	0.3441	0.3563	0.3441	0.3742	0.3852	0.4273	0.4106	0.4652	0.4914
0.8752	0.6769	0.7133	0.7042	0.7106	0.7165	0.6911	0.7435	0.7201	0.7368	0.7821	0.8255	0.8548	0.9133	0.9662
0.9002	1.1202	1.1326	1.0978	1.1436	1.1793	1.1077	1.1770	1.1752	1.2002	1.2468	1.2730	1.3180	1.4075	1.4878
0.9252	1.4800	1.5358	1.5105	1.4786	1.5159	1.4815	1.5649	1.5147	1.5632	1.5920	1.6406	1.6833	1.7871	1.8658
0.9502	1.7441	1.7520	1.7936	1.7503	1.7668	1.7530	1.7800	1.8030	1.7954	1.8083	1.8738	1.9066	1.9889	2.0776
0.9752	1.9172	1.9261	1.9317	1.9150	1.8990	1.8575	1.8658	1.8987	1.9217	1.9110	1.9495	1.9985	2.0693	2.1297
1.0002	1.9481	1.9044	1.9352	1.8827	1.9206	1.8394	1.8850	1.8551	1.9160	1.8917	1.9091	1.9603	2.0248	2.0436
1.0252	1.9266	1.9093	1.8947	1.8611	1.8616	1.8151	1.8285	1.8200	1.8538	1.8260	1.8461	1.8717	1.9061	1.9168
1.0501	1.7924	1.8675	1.8075	1.7923	1.7708	1.7110	1.7569	1.7322	1.7422	1.7350	1.7353	1.7340	1.7519	1.7651
1.0751	1.7462	1.7404	1.6988	1.6454	1.7215	1.6170	1.6342	1.6311	1.6199	1.6211	1.5959	1.6038	1.6059	1.6190
1.1001	1.6571	1.6199	1.6531	1.5844	1.5833	1.5391	1.5491	1.5293	1.5211	1.5190	1.4804	1.5076	1.4808	1.4658
1.1251	1.5553	1.5706	1.5305	1.4746	1.4789	1.4425	1.4399	1.4305	1.4022	1.3957	1.3848	1.3698	1.3560	1.3342
1.1501	1.4911	1.4810	1.4705	1.4113	1.4106	1.3559	1.3503	1.3371	1.3119	1.3103	1.2909	1.2788	1.2527	1.2329
1.1751	1.4231	1.4258	1.3841	1.3447	1.3306	1.2791	1.2775	1.2677	1.2477	1.2342	1.2023	1.1826	1.1541	1.1405
1.2001	1.3503	1.3464	1.3693	1.2632	1.2660	1.2096	1.2158	1.1775	1.1665	1.1547	1.1399	1.1220	1.0821	1.0671
1.2251	1.2979	1.3136	1.2704	1.2416	1.2183	1.1597	1.1752	1.1474	1.1233	1.0961	1.0804	1.0717	1.0243	1.0091
1.2501	1.2491	1.2674	1.2476	1.1819	1.1713	1.1183	1.1136	1.1012	1.0627	1.0415	1.0252	1.0087	0.9757	0.9585
1.2751	1.2106	1.2040	1.1803	1.1538	1.1449	1.0839	1.0849	1.0563	1.0325	1.0137	0.9927	0.9720	0.9351	0.9098
1.3001	1.1814	1.1638	1.1577	1.0987	1.1057	1.0449	1.0531	1.0252	0.9788	0.9788	0.9587	0.9417	0.8983	0.8752
1.3251	1.1445	1.1459	1.1241	1.0883	1.0713	1.0397	1.0247	0.9952	0.9694	0.9406	0.9257	0.9082	0.8749	0.8498
1.3501	1.1127	1.1315	1.1132	1.0825	1.0338	0.9956	0.9902	0.9715	0.9385	0.9291	0.9093	0.8882	0.8521	0.8216
1,3751	1.1065	1.0838	1.0865	1.0634	1.0370	0.9782	0.9718	0.9493	0.9351	0.9049	0.8804	0.8644	0.8318	0.8129
1.4001	1.0883	1.0905	1.0811	1.0328	1.0182	0.9700	0.9669	0.9444	0.9161	0.8961	0.8730	0.8471	0.8207	0.8137
1.4251	1.0796	1.0683	1.0753	0.9966	0.9991	0.9530	0.9519	0.9167	0.9081	0.8802	0.8605	0.8479	0.8165	0.8039
1.4501	1.0596	1.0485	1.0563	1.0067	0.9871	0.9461	0.9363	0.9174	0.9014	0.8713	0.8628	0.8354	0.8091	0.8002

1.4751	1.0631	1.0335	1.0293	1.0051	0.9872	0.9446	0.9500	0.9121	0.8989	0.8650	0.8514	0.8343	0.8147	0.8029
1.5001	1.0485	1.0370	1.0302	0.9938	0.9707	0.9394	0.9422	0.9097	0.8928	0.8704	0.8587	0.8323	0.8264	0.8108
1.5251	1.0356	1.0365	1.0120	0.9787	0.9785	0.9379	0.9330	0.9226	0.8977	0.8717	0.8643	0.8468	0.8321	0.8166
1.5501	1.0325	1.0159	1.0118	0.9889	0.9758	0.9379	0.9361	0.9147	0.8976	0.8720	0.8665	0.8465	0.8418	0.8310
1.5751	1.0153	1.0189	1.0021	0.9955	0.9787	0.9377	0.9321	0.9066	0.9160	0.8828	0.8777	0.8609	0.8657	0.8523
1.6001	1.0219	1.0218	1.0083	0.9991	0.9586	0.9367	0.9441	0.9259	0.9026	0.8921	0.8833	0.8784	0.8822	0.8686
1.6251	1.2044	1.0235	1.0126	0.9791	0.9767	0.9415	0.9415	0.9330	0.9283	0.9056	0.9004	0.8985	0.9004	0.8975
1.6501	1.0127	1.0024	1.0052	0.9949	0.9902	0.9575	0.9600	0.9305	0.9399	0.9273	0.9131	0.9134	0.9181	0.9207
1.6751	1.0280	1.0030	1.0044	0.9887	0.9872	0.9424	0.9633	0.9440	0.9485	0.9369	0.9332	0.9365	0.9413	0.9498
1.7001	1.0056	1.0124	1.0071	0.9959	1.0046	0.9609	0.9767	0.9570	0.9543	0.9459	0.9502	0.9471	0.9684	0.9715
1.7251	1.0123	1.0177	1.0205	0.9966	1.0056	0.9676	0.9922	0.9648	0.9826	0.9721	0.9733	0.9814	0.9946	1.0090
1.7501	1.0262	1.0274	1.0153	1.0045	1.0071	0.9781	0.9980	0.9936	0.9813	0.9832	0.9912	1.0013	1.0157	1.0259
1.7751	1.0231	1.0223	1.0175	1.0223	1.0230	0.9837	1.0110	0.9944	1.0019	1.0098	1.0025	1.0320	1.0403	1.0590
1.8001	1.0298	1.0231	1.0282	1.0205	1.0292	0.9980	1.0243	1.0152	1.0197	1.0115	1.0237	1.0383	1.0570	1.0807
1.8501	1.0254	1.0319	1.0407	1.0167	1.0388	1.0205	1.0447	1.0318	1.0402	1.0541	1.0486	1.0664	1.0920	1.1056
1.9001	1.0309	1.0420	1.0404	1.0377	1.0413	1.0243	1.0642	1.0501	1.0512	1.0571	1.0673	1.0887	1.1025	1.1190
1.9501	1.0357	1.0405	1.0409	1.0371	1.0434	1.0234	1.0509	1.0591	1.0595	1.0602	1.0664	1.0816	1.0844	1.1056
2.0001	1.0213	1.0340	1.0456	1.0324	1.0499	1.0237	1.0618	1.0445	1.0511	1.0619	1.0600	1.0646	1.0696	1.0828
2.0501	1.0288	1.0421	1.0404	1.0372	1.0372	1.0275	1.0572	1.0435	1.0472	1.0430	1.0402	1.0451	1.0488	1.0480
2.1001	1.0246	1.0213	1.0363	1.0256	1.0378	1.0232	1.0403	1.0392	1.0398	1.0331	1.0281	1.0252	1.0214	1.0167
2.1501	1.0115	1.0316	1.0256	1.0209	1.0433	1.0177	1.0380	1.0222	1.0225	1.0133	1.0136	1.0018	1.0041	0.9897
2.2001	1.0233	1.0199	1.0290	1.0177	1.0254	1.0077	1.0175	1.0048	1.0113	0.9970	1.0031	0.9934	0.9839	0.9716
2.2501	1.0137	1.0193	1.0176	1.0160	1.0206	1.0004	1.0123	1.0098	1.0025	0.9991	0.9820	0.9841	0.9735	0.9588
2.3001	1.0124	1.0240	1.0225	1.0135	1.0172	0.9925	1.0092	0.9979	0.9911	0.9895	0.9829	0.9771	0.9672	0.9542
2.3501	1.0133	1.0121	1.0159	0.9918	1.0098	0.9854	1.0065	0.9968	0.9898	0.9849	0.9783	0.9770	0.9634	0.9531
2.4001	1.0250	1.0180	1.0136	1.0130	1.0137	0.9858	1.0069	0.9932	0.9896	0.9811	0.9763	0.9737	0.9681	0.9614
2.4501	1.0020	1.0109	1.0184	1.0007	1.0132	0.9850	0.9978	0.9963	0.9890	0.9824	0.9818	0.9817	0.9730	0.9716
2.5001	1.0082	1.0137	1.0044	1.0005	0.9993	0.9878	0.9981	0.9911	0.9890	0.9856	0.9778	0.9849	0.9830	0.9782
2.5501	1.0099	1.0056	0.9997	1.0044	1.0108	0.9867	0.9999	0.9933	0.9915	0.9852	0.9857	0.9897	0.9915	0.9957
2.6001	1.0005	1.0032	1.0055	0.9949	1.0123	0.9896	1.0080	0.9960	0.9923	0.9912	0.9934	0.9919	0.9984	0.9971
2.6501	1.0061	1.0091	1.0017	0.9979	1.0083	0.9877	1.0129	1.0020	1.0022	1.0007	0.9954	1.0027	1.0038	1.0079
2.7001	1.0075	1.0047	1.0015	0.9930	1.0122	0.9889	1.0111	1.0041	1.0010	0.9995	1.0016	1.0051	1.0102	1.0165
2.7501	0.9962	1.0093	1.0126	1.0039	1.0020	0.9965	1.0171	1.0024	1.0035	1.0026	1.0036	1.0109	1.0147	1.0228
2.8001	1.0139	1.0026	1.0035	1.0073	1.0063	0.9947	1.0181	1.0090	1.0099	1.0050	1.0030	1.0097	1.0133	1.0246
2.8501	1.0057	1.0071	1.0104	1.0054	1.0081	0.9892	1.0175	1.0028	1.0016	1.0076	1.0039	1.0104	1.0136	1.0204
2.9001	1.0013	1.0075	1.0036	1.0048	1.0109	0.9918	1.0194	1.0023	1.0100	1.0028	1.0032	1.0030	1.0113	1.0145

TABLE I (*continued*)

	Density in units of 10^{27} atoms/m^3													
R/Rm	2.000	2.500	3.000	4.000	5.000	6.000	7.000	8.000	9.000	10.000	11.000	12.000	13.000	14.000
2.9501	1.0092	1.0150	0.9947	0.9976	1.0047	0.9990	1.0145	1.0048	1.0072	1.0125	1.0018	1.0085	1.0097	1.0090
3.0001	1.0082	1.0059	1.0046	1.0007	1.0075	0.9949	1.0115	1.0040	1.0015	1.0043	1.0056	1.0042	1.0028	0.9988
3.0501	1.0045	1.0056	1.0060	0.9982	1.0055	0.9972	1.0125	1.0000	1.0013	1.0065	1.0000	1.0027	0.9970	0.9988
3.1001	1.0078	1.0050	0.9995	1.0023	1.0089	0.9903	1.0088	0.9970	1.0039	0.9999	0.9971	0.9966	0.9966	0.9959
3.1500	0.9997	1.0082	1.0035	0.9995	1.0079	0.9992	1.0104	1.0019	1.0010	0.9980	0.9985	0.9979	0.9939	0.9901
3.2000	1.0008	0.9994	0.9947	1.0013	1.0066	0.9975	1.0050	0.9996	0.9997	0.9928	0.9943	0.9940	0.9920	0.9884
3.2500	0.9993	0.9990	1.0030	1.0003	1.0041	0.9990	1.0014	0.9967	0.9954	0.9965	0.9954	0.9980	0.9917	0.9889
3.3000	1.0022	1.0089	1.0002	0.9966	1.0057	0.9905	1.0076	0.9991	0.9995	0.9965	0.9971	0.9977	0.9959	0.9891
3.3500	1.0068	1.0006	1.0020	0.9942	1.0074	0.9995	1.0020	0.9977	0.9988	0.9978	0.9956	0.9993	0.9949	0.9914
3.4000	1.0022	1.0051	1.0006	0.9972	1.0027	0.9950	1.0070	0.9938	0.9965	0.9926	0.9964	0.9978	0.9978	0.9951
3.4500	0.9966	1.0001	0.9993	0.9959	1.0064	0.9925	1.0033	1.0023	0.9997	0.9938	0.9991	1.0008	1.0013	1.0022
3.5000	0.9980	1.0051	1.0000	0.9995	1.0034	0.9918	1.0054	0.9992	0.9937	0.9963	1.0004	0.9985	1.0010	1.0034
3.5500	1.0025	1.0102	1.0064	0.9876	1.0058	0.9935	1.0050	1.0002	1.0010	0.9960	1.0027	1.0047	1.0012	1.0013
3.6000	0.9985	1.0022	0.9976	0.9957	1.0014	0.9971	1.0075	1.0018	0.9989	0.9975	1.0042	1.0026	1.0022	1.0027
3.6500	0.9974	1.0016	0.9937	0.9925	0.9994	0.9906	1.0047	1.0009	0.9983	1.0013	0.9989	1.0002	1.0028	1.0028
3.7000	0.9942	1.0005	1.0011	0.9927	1.0047	0.9936	1.0045	0.9997	1.0013	0.9995	0.9998	1.0013	1.0014	1.0039
3.7500	0.9968	1.0075	0.9987	0.9908	1.0004	0.9958	1.0043	0.9969	1.0022	0.9974	1.0005	0.9960	1.0004	1.0020
3.8000	1.0044	0.9966	0.9982	0.9956	1.0011	0.9986	1.0084	1.0004	1.0024	1.0039	0.9990	0.9993	1.0006	1.0014
3.8500	0.9976	1.0019	0.9961	0.9956	1.0026	0.9998	1.0026	1.0000	1.0026	1.0041	1.0000	1.0038	0.9989	1.0018
3.9000	1.0026	0.9988	0.9988	0.9914	1.0069	0.9982	1.0059	0.9988	1.0071	1.0023	1.0007	1.0021	0.9997	1.0003
3.9500	1.0007	1.0004	0.9934	0.9969	1.0018	0.9966	1.0054	0.9962	0.0051	1.0021	0.9976	1.0029	1.0004	0.9980
4.0000	0.9959	1.0021	0.9956	0.9978	1.0044	0.9977	1.0028	0.9998	1.0049	0.9987	1.0002	1.0014	0.9979	1.0003
4.0500	0.9971	0.9993	0.9939	0.9967	1.0053	0.9985	1.0068	0.9973	1.0003	0.9953	1.0008	0.9973	1.0001	0.9975

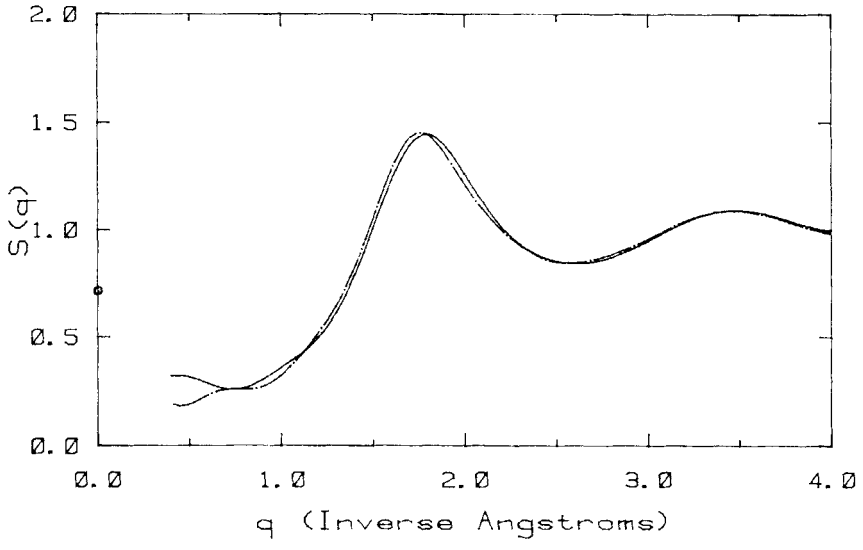

(a)

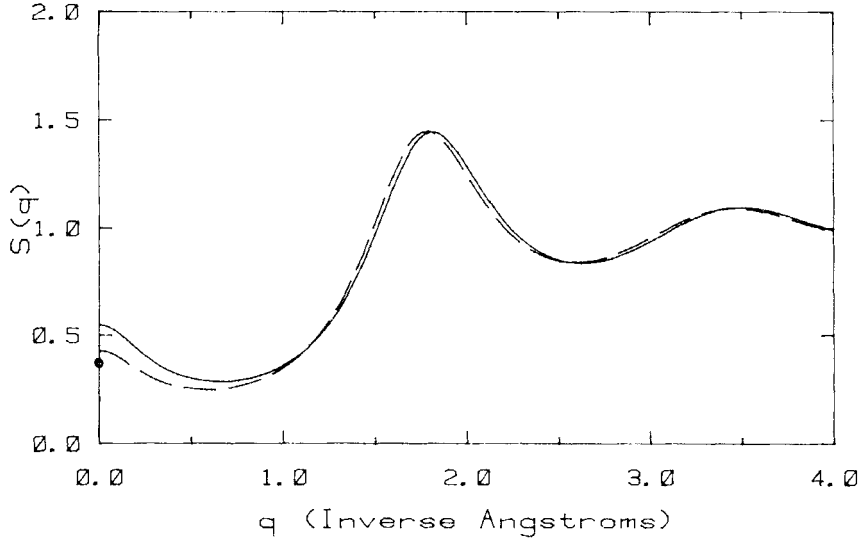

(b)

FIGURE 3 (a) The same as Figure 2 but for $\rho = 11 \times 10^{27}$ atoms/m^3. (b) The same as Figure 1b but for $\rho = 11 \times 10^{27}$ atoms/m^3.

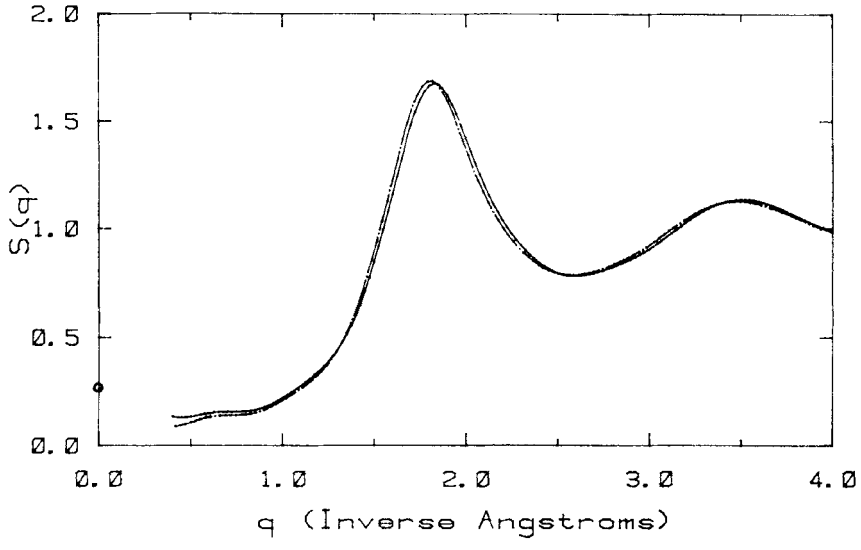

(a)

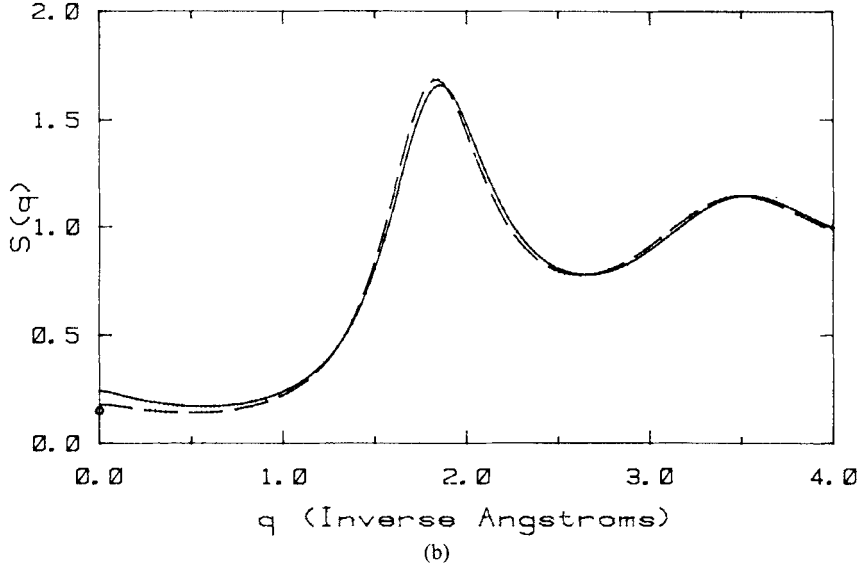

(b)

FIGURE 4 (a) The same as Figure 2 but for $\rho = 14 \times 10^{27}$ atoms/m^3. (b) The same as Figure 1b but for $\rho = 14 \times 10^{27}$ atoms/m^3.

data shown in Figure 1. For Figures 3 and 4 the two Monte Carlo results are compared in part (a) while the PY results are compared in part (b). From Figures 1 and 2 it is seen that if we compare either the Monte Carlo or PY results for both the potentials we reach the same conclusion as discussed in Section II. The circle on the $S(q)$ axis shows the value of $S(o)$. It is evident that at $\rho = 6 \times 10^{27}$ atoms/m^3 there is a substantial peak at the origin similar to that shown in Figure 1 for the PY data.

In Figures 3a and 3b we note that, unlike Figures 1 and 2, the peak positions for the MC and PY results are different. The PY peaks are shifted to higher q by about 0.1 Å^{-1}. Relatively large differences are observed at low q with similar conclusions as for Figures 1 and 2. In Figures 4a and 4b peak shifts between MC and PY results are seen, and at low q similar relative differences to Figure 3a. In both cases the MC data show a larger $q \to 0$ limit than the PY data.

The conclusions from data shown in these curves for $\rho = 6 \times 10^{27}$ atoms/m^3 are in qualitative agreement with those drawn from data at lower density, either published[1,2] or obtained in this investigation. However at the lower densities we may use a virial expansion for $S(q)$ to obtain reliable results at low q, and also the differences between MC and PY results vanish at low ρ.

B Thermodynamic functions

The thermodynamic functions can be expressed in terms of the radial distribution functions with the following equations:

$$\beta \frac{P}{\rho} = 1 - \frac{2\pi\rho}{3} \int_0^\infty r^3 \beta \frac{\mathrm{d}u(r)}{\mathrm{d}r} \, g(r) \, \mathrm{d}r \tag{6}$$

$$kT\left(\frac{\partial \rho}{\partial P}\right)_T = 1 + 4\pi\rho \int_0^\infty r^2[g(r) - 1] \, \mathrm{d}r \tag{7}$$

and from Eqs (5) and (7)

$$S(q = 0) = kT\left(\frac{\partial \rho}{\partial P}\right)_T = \rho kT\chi \tag{8}$$

where P is the pressure and χ the isothermal compressibility. The integral in Eq. (6) was evaluated by using a one-interval 16 point Gaussian integration, and the integrand was divided into a number of intervals. We have checked the accuracy of our evaluation by using different upper limits of integration. On the basis of these calculations, 11 intervals and an upper limit of $R(=r/R_m) = 10$ were used to evaluate the integral. We estimate the numerical error to be ± 0.015.

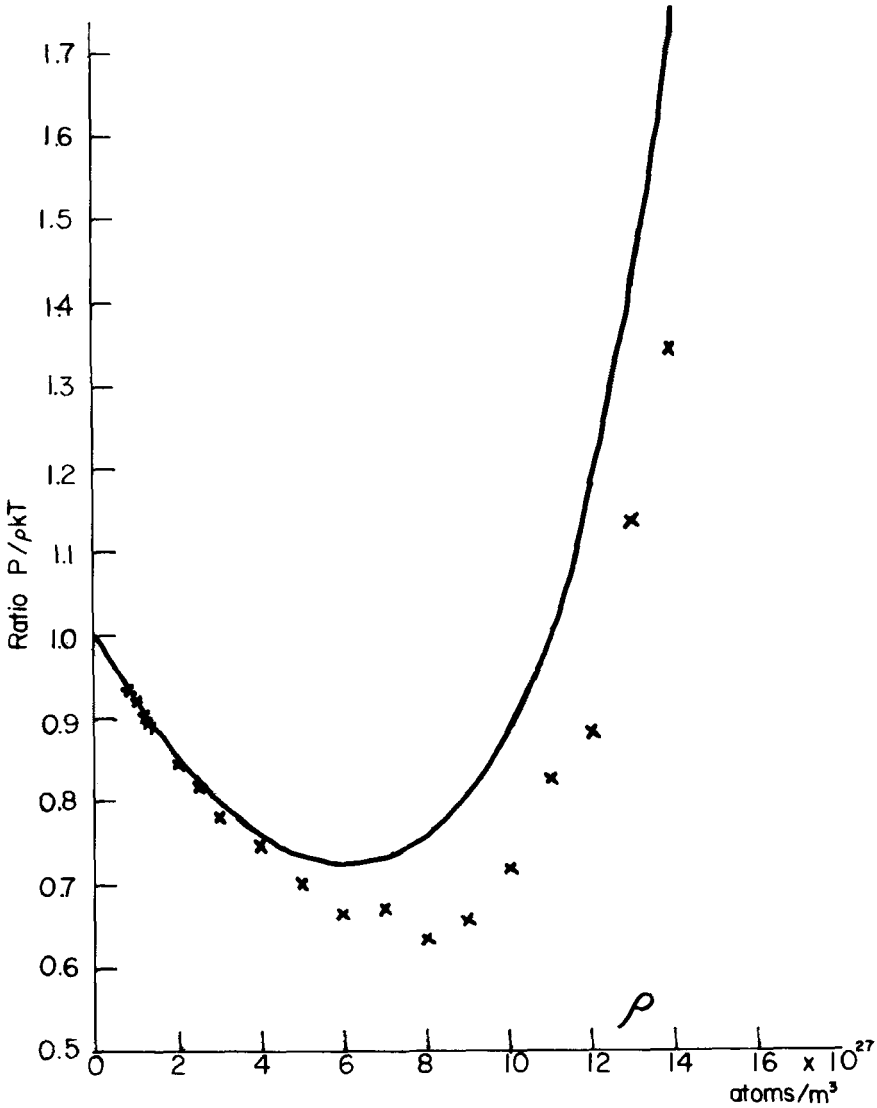

FIGURE 5 Equation of state of a Barker *et al.*[7] fluid at $T = 297$ K. Crosses are the Monte Carlo results; full line, experimental data. In addition to the densities used in our calculations ($\rho \geq 2 \times 10^{27}$ atoms/m^3) we have shown data at lower ρ taken from a previous paper.[14]

The pressures obtained from the Barker *et al.* potential and Eq. (6) are plotted in Figure 5, and for $\rho > 3 \times 10^{27}$ atoms/m^3 there are significant differences from the experimental data showing the relative importance of many body forces to this property. By contrast the PY pressures are in good agreement with the experimental values, as shown by the differences plotted in Figure 6. Thus in this case the error in the PY approximation fortuitously accounts for the many body potential terms. Finally we show in Figure 6 a line representing the equation $c\rho^2$, where the coefficient c is determined from the three body potential term in the third virial coefficient of the pressure. The general agreement suggests that the higher terms mutually cancel.

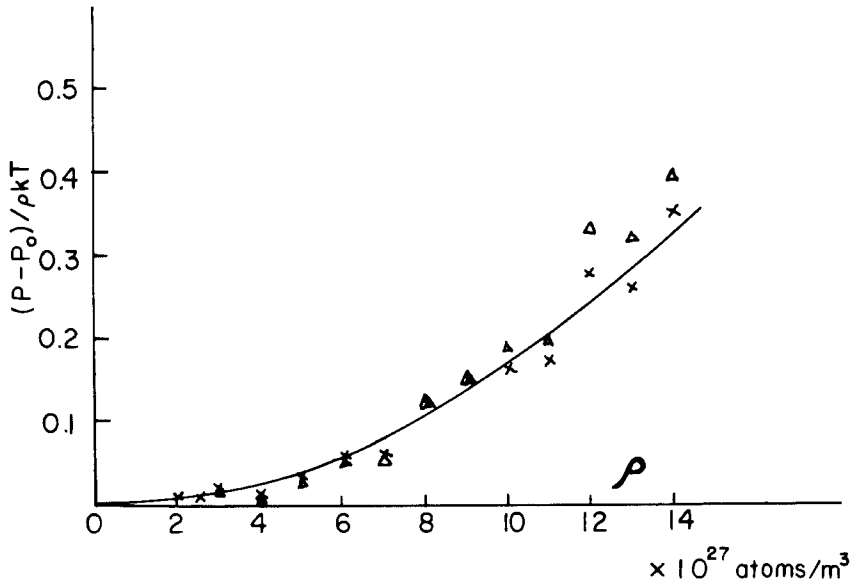

FIGURE 6 Pressure differences at $T = 297$ K. Crosses, experimental curve minus MC data from Figure 5. Triangles are similar results for PY minus MC data. Full line is extrapolation of 3rd virial coefficient term from low to high density.

By smoothing and then differentiating the MC data in Figure 5, we have obtained $\partial\rho/\partial P|_T$, and used Eq. (8) to find χ and $S(o)$. Conclusions from these results are essentially the same as discussed above, and the values of $S(o)$ are shown in Figures 2, 3a and 4a. In Figures 1, 3b and 4b the $S(o)$'s obtained in the same way but using the PY $g(r)$'s are shown by circles.

IV STRUCTURE FACTORS IN THE PRESENCE OF THREE-BODY FORCES

For the purpose of investigating the effect of three-body interactions on the structure of fluids, we used the effective potential of Sinha *et al.*[11] which is given in reduced form as

$$u^{*\text{eff}}(R_{12}) = u^*(R_{12}) - \frac{2\pi}{R_{12}}\rho^* T^* \int_0^\infty \int_{|R_{12}-R_{13}|}^{R_{12}+R_{13}} g_0(R_{12}) g_0(R_{13}) \times \{\exp[-u^*(123)/T^*] - 1\} R_{13} R_{23}\, dR_{13}\, dR_{23} \tag{9}$$

where $g_0(R_{ij})$ is the true pair potential radial distribution function, $u^*(R_{ij})$ $(=u/\varepsilon)$ the reduced interaction energy between the particles of an isolated pair, $\rho^*(=\rho R_m^3)$ is the reduced number density, $T^*(=kT/\varepsilon)$ the reduced temperature and $u^*(1, 2, 3)$ is the reduced three-body nonadditive interaction given as

$$u^*(1, 2, 3) = Z^*_{111} W_{111}(1, 2, 3) + Z^*_{112} W_{112}(1, 2, 3) + Z^*_{121} W_{121}(1, 2, 3) + Z^*_{211} W_{211}(1, 2, 3). \tag{10}$$

In Eq. (10) the subscripts 1 and 2, respectively, indicate the interactions arising due to dipole and quadrupole. Each Z^* in (10) is an integration constant in dimensionless form depending on the atomic species. Since all three atoms 1, 2, 3 are identical,

$$Z^*_{112} = Z^*_{121} = Z^*_{211}.$$

The function $W_{ijk}(1, 2, 3)$ is given by

$$W_{111} = 3(R_{12} R_{23} R_{31})^{-3}[1 + 3\cos\gamma_1 \cos\gamma_2 \cos\gamma_3] \tag{11}$$

$$W_{121} = \tfrac{3}{16}(R_{12} R_{23})^{-4} R_{31}^{-3}[9(\cos\gamma_2 - 25\cos 3\gamma^2) + 6\cos(\gamma_1 - \gamma_3)(3 + 5\cos 2\gamma_2)] \tag{12}$$

The γ's are the interior angles of the three-particle triangle and are related to the integration variables according to the cosine law, as

$$\gamma_1 = \arccos[(R_{12}^2 + R_{13}^2 - R_{23}^2)/2\, R_{12} R_{13}]$$

$$\gamma_2 = \arccos[(R_{12}^2 + R_{23}^2 - R_{13}^2)/2\, R_{12} R_{23}]$$

$$\gamma_3 = \arccos[(R_{23}^2 + R_{13}^2 - R_{12}^2)/2 R_{23} R_{13}] \tag{13}$$

The effective potential is evaluated using the krypton potential of Barker *et al.* and its Monte Carlo values for the radial distribution function at $T =$ 297 K and $\rho = 14 \times 10^{27}$ atoms/m^3. The values of the integration constants

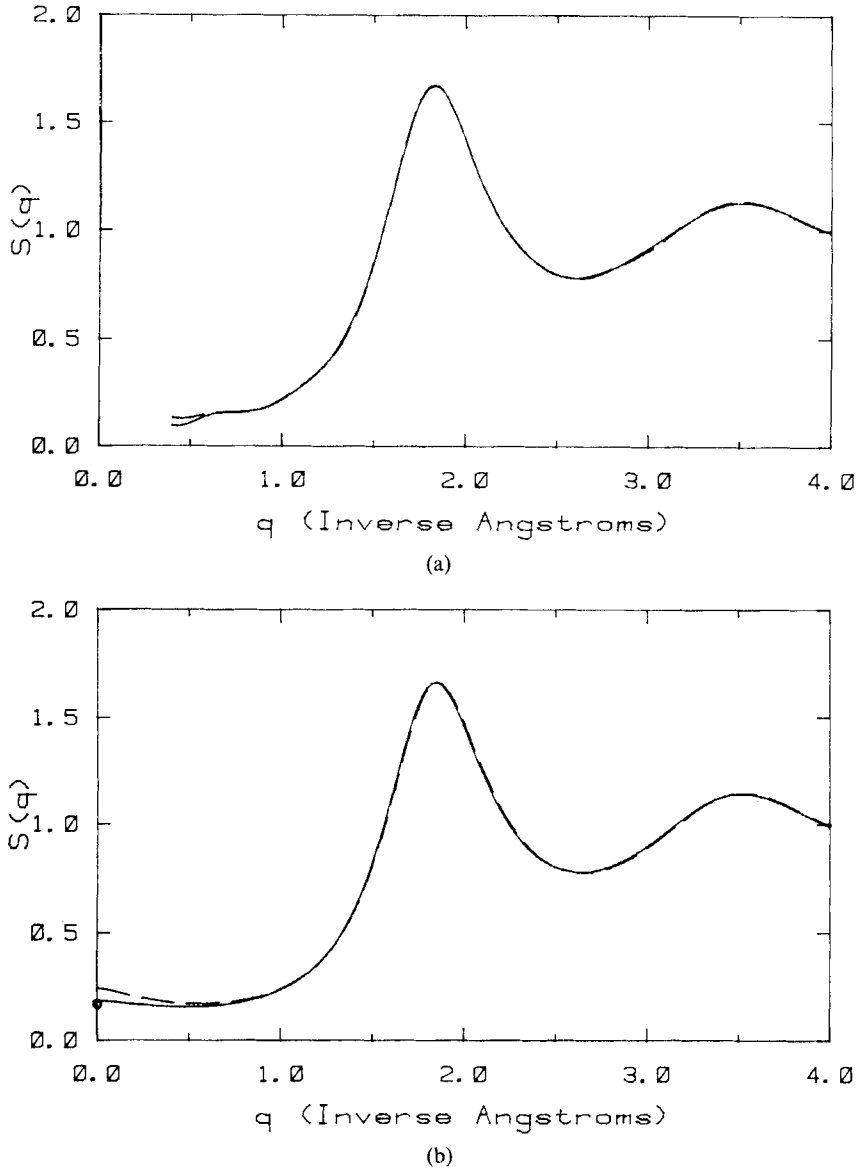

FIGURE 7 Monte Carlo and Percus–Yevick structure factors for krypton at 297 K and $\rho = 14 \times 10^{27}$ atoms/m^3. (a) Monte Carlo simulation with the Barker *et al.* pair potential – – dash line. Monte Carlo simulation using an effective potential obtained by adding triple dipole and double dipole-quadrupole terms to the former potential — full line. (b) Percus–Yevick solution using Barker *et al.* pair potential – – dash line. Percus–Yevick solution using an effective potential discussed above — full line. The circle on $S(q)$ axis shows the value of $S(o)$ obtained in section IIIB.

used are due to Bell[12] for krypton, given as

$$Z^*_{111} = 0.010281; Z^*_{121} = 0.000694 \tag{14}$$

The Monte Carlo calculation was done using the numerical values of this effective potential. Though this effective potential is state dependent the advantage of using this is, once the effective potential is evaluated it takes the same time in Monte Carlo calculations as in the case of the usual two-body computations. On the other hand the calculations including the triplet interactions required 15 times more computer time than that for the usual computations based on the pair potential.

The resulting Monte Carlo and PY structure factors are plotted in Figure 7. From comparison with the two-body results we notice that except at low values of q the effect of three-body forces on the structure factor is negligible, and that there is a general similarity between Figures 7 and 4 in spite of the addition of the 3-body potential.

Recently Ram *et al.*[11,13] have made a systematic study using an integral equation perturbation theory to see the effect of three-body nonadditive dispersion interactions on the equilibrium properties of argon and xenon. They have found that its effect on the radial distribution function is negligibly small at high densities.

V CONCLUSIONS

We have made Monte Carlo simulations of a system of atoms and numerical solutions of the Percus–Yevick equation at room temperature interacting with the Lennard-Jones (12–6) potential, krypton potential of Barker *et al.*, and a long range three-body (triple dipole and dipole-dipole-quadrupole) potential. The object has been to find the relevant part of $u(r)$ and $S(q)$ for the comparisons of absolute values with experiment and to investigate the effect of a long range three-body potential on $g(r)$ and $S(q)$. In the case of the pressure the MC data using the Barker *et al.* potential showed significant differences from experiment, while the PY values were in agreement.

In comparisons of Lennard-Jones and Barker *et al.*, krypton potentials and their Monte Carlo and PY structure factors, we found that if the point where $u(r) = 0$ is chosen appropriately either potential would yield a reasonable fit to the data for $q > 2$ Å^{-1}. Also we have found that except at low values of q the effect of three-body forces on the structure factor is negligible at the state studied here.

This investigation has consolidated previous investigations[2,14] and established the importance of densities near 6×10^{27} atoms/m^3 and $q < 1$ Å^{-1} in the study of effects related to three body and higher forces.

References

1. A. Teitsma and P. A. Egelstaff, *Phys. Rev.* **A21**, 367, 1980.
2. P. A. Egelstaff, A. Teitsma and S. S. Wang, *Phys. Rev.* **A22**, 1702, 1980.
3. J. P. Hansen and J. R. McDonald, *Theory of Simple Liquids*, Academic Press (London, 1976).
4. B. M. Axilrod and E. Teller, *J. Chem. Phys.* **11**, 299, 1943.
5. P. A. Egelstaff and A. Teitsma, *Phys. Rev. Lett.* **43**, 503, 1979.
6. J. A. Barker and D. Henderson, *Rev. Mod. Phys.* **48**, 587, 1976.
7. J. A. Barker, R. O. Watts, J. K. Lee, T. P. Schafer and Y. T. Lee, *J. Chem. Phys.* **61**, 3081, 1974.
8. P. A. Egelstaff, W. Gläser, D. Litchinsky, E. Schneider and J. B. Suck, *Phys. Rev. A*, **27**, 1106, 1983.
9. A. A. Broyles, *J. Chem. Phys.* **33**, 456, 1960.
10. G. G. Chell and I. J. Zucker, *J. Phys.* **C1**, 35, 1968.
11. S. K. Sinha, J. Ram and Y. Singh, *J. Chem. Phys.* **66**, 5013, 1977.
12. R. J. Bell, *J. Phys.* **B3**, 751, 1970.
13. J. Ram, S. K. Sinha and Y. Singh, *J. Chem. Phys.* (to be published).
14. J. Ram, R. Barker, P. T. Cummings and P. A. Egelstaff, *Phys. Chem. Liq.* **11**, 315, 1982.